

## High-temperature $^{63}\text{Cu}(2)$ nuclear quadrupole and magnetic resonance measurements of $\text{YBa}_2\text{Cu}_4\text{O}_8$

N. J. Curro

*Department of Physics and Materials Research Laboratory, University of Illinois at Urbana-Champaign, 1110 West Green Street, Urbana, Illinois 61801-3080*

T. Imai

*Department of Physics, #13-3149, Massachusetts Institute of Technology, Cambridge, Massachusetts 02139*

C. P. Slichter\*

*Department of Physics and Materials Research Laboratory, University of Illinois at Urbana-Champaign, 1110 West Green Street, Urbana, Illinois 61801-3080*

B. Dabrowski

*Department of Physics, Northern Illinois University, De Kalb, Illinois 60115*

(Received 15 August 1996; revised manuscript received 6 March 1997)

We report data on the Gaussian transverse relaxation rate  $1/T_{2G}$ , the Knight shift  $K^s$ , and the spin-lattice relaxation time  $T_1$ , in  $\text{YBa}_2\text{Cu}_4\text{O}_8$  from 100 K up to 715 K, extending the upper temperature of previous studies by 200 K. The  $T_{2G}$  data are corrected for a small spin-lattice fluctuation contribution to the echo decay. Calculations of  $T_1T/T_{2G}$  and  $T_1T/T_{2G}^2$  show that there is a crossover in scaling behavior at a temperature  $T_{cr} \sim 500$  K. The Knight-shift data also exhibit a maximum at this temperature and decrease slowly with increasing temperature above this. Calculations using an independent form for the susceptibility due to Sokol, Singh, and Elstner suggest that the correlation length for antiferromagnetic fluctuations is on the order of one to two lattice spacings at this crossover temperature, in agreement with the proposal of Barzykin and Pines. [S0163-1829(97)04526-8]

### INTRODUCTION

We have measured the nuclear quadrupole resonance (NQR) spin-lattice relaxation rate  $1/T_1$ , the NQR spin-spin relaxation rate  $1/T_{2G}$ , and the nuclear magnetic resonance (NMR) shift  $K$  of the planar  $^{63}\text{Cu}$  in  $\text{YBa}_2\text{Cu}_4\text{O}_8$  between 77 and 715 K. Although this material has been studied extensively by other groups,<sup>1-3</sup> no data on  $1/T_{2G}$ , or the Knight shift above 500 K have been reported previously, to our knowledge. We extend the data to higher temperatures and confirm a recent conjecture made by Barzykin and Pines<sup>4</sup> concerning the magnetic scaling behavior of this material at high temperatures. Specifically, our data support the hypothesis that the electronic spin system crosses over from a quantum critical (QC)  $z=1$  scaling regime to a nonuniversal mean-field regime with  $z=2$  when the temperature exceeds  $T_{cr} \sim 500$  K. Furthermore, we find that Knight shift reaches a maximum at this temperature.

### EXPERIMENT

The sample is an unaligned powder with a room-temperature NQR linewidth of 190 kHz at full width half maximum. It was prepared as described in Ref. 5. The superconducting transition temperature was measured to be 79 K using a superconducting quantum interference device magnetometer. These quantities are comparable to those of a sample studied previously<sup>3</sup> which had a transition temperature of 81 K and a NQR linewidth of 160 kHz. An unaligned

powder was necessary because the epoxy used to form aligned samples limits the upper temperature at which measurements can be performed to about 500 K. A magnetically shielded probe designed for high-temperature studies was used for all of the NQR measurements to eliminate errors from ambient magnetic fields (see below). The spin-lattice relaxation rates,  $1/T_1$ , were obtained with the standard inversion recovery pulse sequence and the data were fit to a single exponential recovery function, as described elsewhere.<sup>3</sup> The data are shown in Figs. 1(a) and 1(b). For comparison the data of Corey *et al.* are shown, which go only up to 500 K. The new data agree well with the previous measurements and extend up to 715 K.

For the spin-spin relaxation times, the envelope of the echo decay was measured using a  $90-\tau-180$  pulse sequence and the Gaussian part of the decay,  $T_{2G}$ , was extracted by fitting to the function:

$$S(2\tau) = S(0)e^{-2\tau/T_{2R}}e^{-(2\tau)^2/2T_{2G}^2}f(2\tau). \quad (1)$$

Here  $f(2\tau)$  is a contribution to the echo decay caused by spin-lattice fluctuations. Echo decays for the planar Cu in the high- $T_c$  materials traditionally have been interpreted under the assumption that the neighboring spins remain static during the time scale of the echo decay. In the Appendix we show that there is a small spin-lattice contribution in  $\text{YBa}_2\text{Cu}_4\text{O}_8$  which can be corrected for. This correction is typically of the order of 1–3%, and does not qualitatively

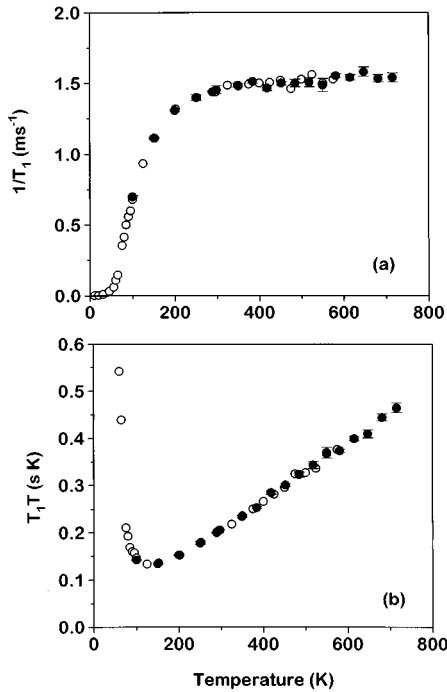


FIG. 1. (a)  $^{63}\text{Cu}(2)$  spin-lattice relaxation rate  $1/T_1$  as a function of temperature. (b)  $T_1T$  as a function of temperature. The open circles are the data of Corey *et al.* (Ref. 3) and the solid circles are from the present study.

affect the temperature dependence of  $T_{2G}$ .  $T_{2R}$  is the Lorentzian or Redfield part of the decay, which is set independently by the relation

$$\frac{1}{T_{2R}} = \frac{(\beta + R)}{T_1}, \quad (2)$$

where  $R$  is the anisotropy ratio and  $\beta = 2$  for NQR. We have used the value 3.3 for  $R$ .<sup>6</sup> We found that we could fit the data adequately at all temperatures with this procedure, and did not have to include any extra Lorentzian components at higher temperatures. Figure 2 shows a typical data set for which this Lorentzian part has been divided out. The data show clear Gaussian behavior extending over one and a half decades of signal intensity. Figure 3 shows  $T_{2G}$  as a function of temperature up to 715 K.

Measurements of the intrinsic value of spin-echo decay time  $T_{2G}$  can be obscured easily by spurious effects. Previous studies<sup>3</sup> reported that the NQR  $T_{2G}$  is depressed by the presence of small ambient fields on the order of a few Gauss. In order to verify this effect, we undertook a systematic measurement of  $T_{2G}$  in a known external field. A solenoid was constructed which applied a static field along the  $H_1$  direction (the axis of the coil). The whole assembly was then surrounded by magnetic shielding to minimize uncertainties about the ambient fields in the laboratory. The spin-echo decay was measured as a function of the dc current in the solenoid. The solenoid field  $B$  was determined using the relation

$$B = \mu_0 NI, \quad (3)$$

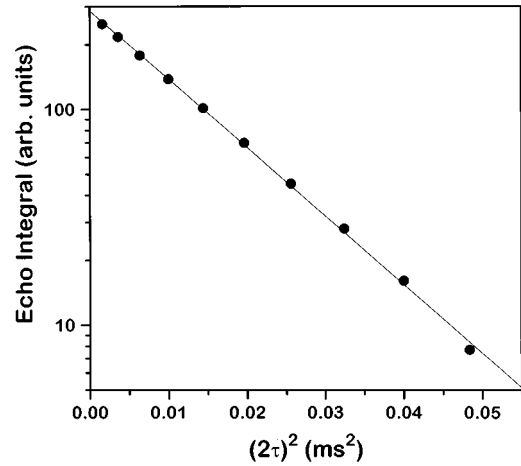


FIG. 2. Logarithm of the  $^{63}\text{Cu}(2)$  NQR echo integral as a function of  $(2\tau)^2$  where  $\tau$  is the spacing between the  $90^\circ$  and  $180^\circ$  pulses demonstrating the Gaussian character of the decay. The Lorentzian component has been divided out.

where  $\mu_0$  is the permeability of free space,  $I$  is the dc current, and  $N$  is the number of turns per unit length. As seen in Fig. 4, even a field as low as 1–2 G can depress the measured value significantly. The solid line in the graph is a fit to the equation<sup>7</sup>

$$T_{2G}^{-2}(B) = C(^{63}\gamma B)^2 + T_{2G}^{-2}(0), \quad (4)$$

where  $^{63}\gamma$  is the gyromagnetic ratio of copper, and  $C$  is a fit parameter of order unity. The quality of this fit justifies corrections to  $T_{2G}$  based on this formula made in previous studies.<sup>3</sup> Furthermore, the data extrapolated to the zero-field value agree with the value measured with the magnetic shielding in place. The  $T_{2G}$  data below room temperature were taken in a nitrogen dewar which was not magnetically shielded, so the measured values were corrected using this formula.

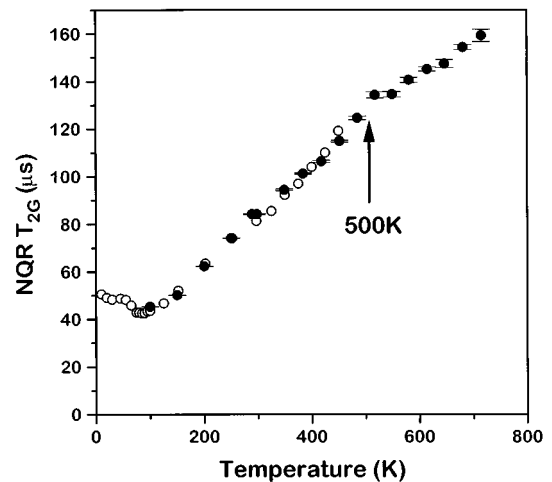


FIG. 3.  $^{63}\text{Cu}(2)$  NQR  $T_{2G}$  as a function of temperature. The open circles are the data of Corey *et al.* (Ref. 3) and the solid circles are from the present study. The data shown here have not been corrected for spin-lattice contributions.

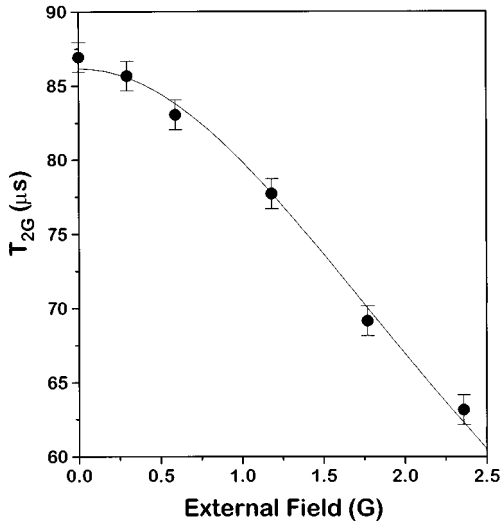


FIG. 4. The NQR  $T_{2G}$  as a function of an applied static magnetic field. The solid line is a fit to Eq. (4).

$T_{2G}$  can also be affected by the size of the radio-frequency excitation pulses  $H_1$  relative to the linewidth. For the case in which  $H_1$  is less than the linewidth,  $T_{2G}$  has been observed<sup>8</sup> to increase with increasing  $H_1$  in  $\text{YBa}_2\text{Cu}_3\text{O}_{7-\delta}$ . Corey *et al.* report that the NQR  $T_{2G}$  in  $\text{YBa}_2\text{Cu}_4\text{O}_8$  is independent of  $H_1$  for  $H_1$  values greater than  $\sim 70$  kHz. In this study, we find similar behavior, and all measurements were performed in the regime where  $T_{2G}$  is independent of  $H_1$ . We thus feel confident that our measured  $T_{2G}$  values truly reflect the intrinsic properties of the system.

Our previous studies of  $\text{YBa}_2\text{Cu}_4\text{O}_8$  at high temperatures<sup>3</sup> were limited by anomalous effects seen in the data above 450 K. Specifically we found a sudden drop in the measured  $T_{2G}$ , as well as changes in the line shape above this temperature. We believe that the anomalous behavior above 500 K in the previous sample was due to some extrinsic effect, perhaps from aging or thermal cycling. In the present study using a different sample we see none of these effects, although there is a reproducible change in the slope of  $T_{2G}$  above 500 K. In the new sample, though, there were no accompanying changes in either  $1/T_1$  or the line shape. We believe that the present sample shows no anomalous extrinsic behavior, and that the change in slope at 500 K is an intrinsic effect brought about by changes in the electronic system, as discussed below.

The measurements of the magnetic shift  $K$  were made in a field of 8.31 T using a nitrogen dewar for temperatures between 77 K and room temperature, and a laboratory-built high-temperature probe for temperatures up to 700 K.  $K$  is actually the sum of the temperature-independent orbital shift  $K^{\text{orb}}$ , and the Knight shift  $K^{\text{S}}(T)$ . For the  $c$  axis parallel to the static field  $H_0$ , the sum of the hyperfine constants,  $A_{\parallel} + 4B$ , is approximately zero and consequently there is no significant temperature dependence to  $K_{\parallel}$ .  $A$  and  $B$  are the on-site and nearest-neighbor hyperfine constants for the Cu nucleus in the Mila-Rice Hamiltonian.<sup>9</sup> When the field is oriented perpendicular to the  $c$  axis, however, the sum of the hyperfine constants does not vanish. Thus by measuring  $K_{\perp}(T)$ , one can measure the temperature dependence of the

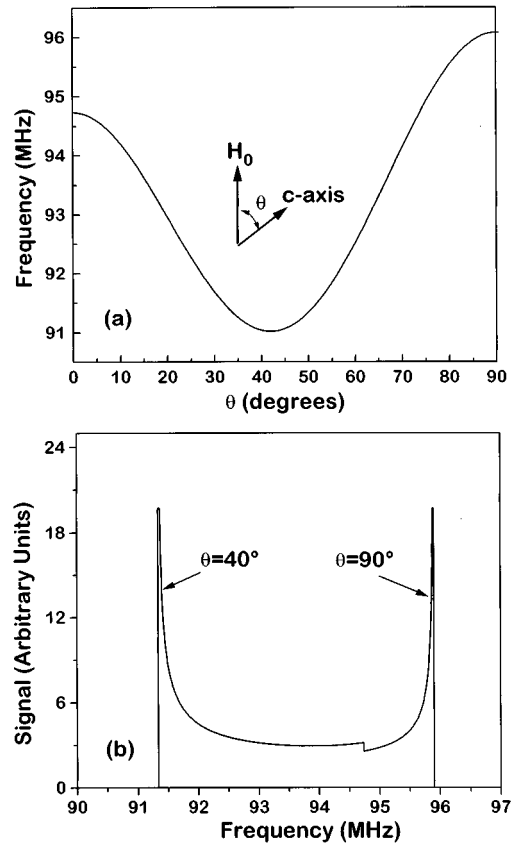


FIG. 5. (a) The resonance frequency for the  $^{63}\text{Cu}(2)$  central transition as a function of the angle between the  $c$  axis of the crystal and the applied field. (b) The characteristic powder pattern for the NMR absorption strength versus frequency, given the angular dependence of the NMR line position.

uniform spin susceptibility,  $\chi_0(T)$ . Ideally this measurement would be done using single crystals or an oriented powder by simply aligning the  $c$  axis of the sample perpendicular to the field. Unfortunately the epoxy commonly used for oriented powders, Stycast 1266, oxidizes above  $\sim 500$  K precluding any high-temperature studies. Furthermore, no single crystals of  $\text{YBa}_2\text{Cu}_4\text{O}_8$  of sufficient size were available to us. Thus in order to measure  $K_{\perp}(T)$  we measured the temperature dependence of the powder pattern and from this extracted the shift.

Figure 5 illustrates this method. Panel (a) shows the  $^{63}\text{Cu}(2)$  resonance frequency of the central transition as a function of the angle,  $\theta$ , between the  $c$  axis of the crystallite and the field  $\mathbf{H}_0$ . The frequency change with angle results from a combination of quadrupole coupling and Knight-shift anisotropy. Panel (b) shows the characteristic spectrum that arises for a random distribution of angles. The singularity, or ‘‘horn,’’ at the upper end corresponds to crystallites oriented perpendicular to the field. By measuring the position of this horn one can study the magnetic shift  $K_{\perp}$  selectively. Experimentally, this singularity is washed out because of a distribution of quadrupole frequencies. This effect is mathematically equivalent to convoluting the spectrum with a Gaussian function. Figure 6 shows the experimental point by point frequency spectrum, and a fit to a convoluted powder pattern. The dotted line shows the ideal (unconvoluted) spectrum.

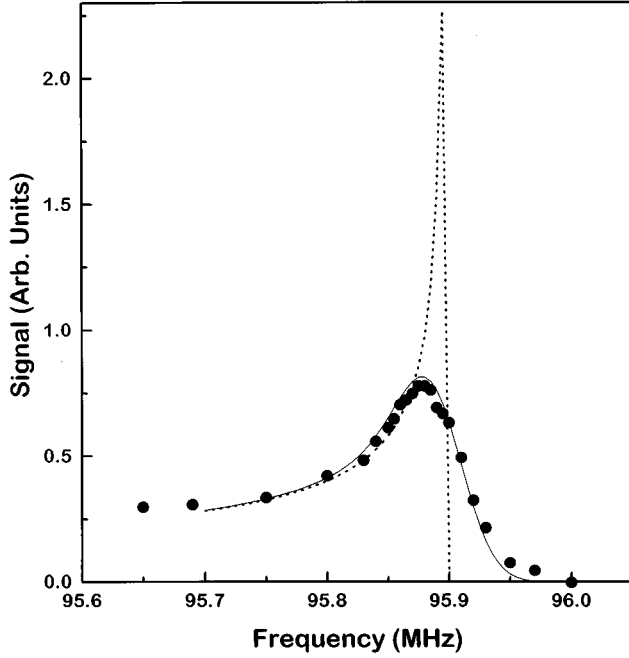


FIG. 6. The experimental frequency spectrum showing the horn at  $90^\circ$ . The solid circles are the data at 475 K with the baseline subtracted, the dotted line is the ideal powder pattern in the absence of NQR broadening, and the solid line is powder pattern which has been convoluted with a Gaussian distribution.

One can see that the convolution displaces the position of the singularity to lower frequencies. To measure the true magnetic shift one must account for this offset. We found that we could fit our spectra by convolution with a Gaussian of width

$$w = \frac{\partial A}{\partial \nu_Q} \Delta \nu_Q = \frac{3 \nu_Q}{8 \nu_0} \Delta \nu_Q, \quad (5)$$

where  $A$  is the second-order correction to the central transition due to the quadrupolar coupling,<sup>10</sup>  $\nu_Q(T)$  is the NQR frequency,  $\nu_0$  is the Larmor frequency, and  $\Delta \nu_Q$  is the Gaussian width of the NQR resonance. The offset in frequency was then determined and added to the measured peak position. One can then proceed to calculate the magnetic shift using the exact formula for the perpendicular central transition frequency:

$$\begin{aligned} \nu_\perp(T) = & \frac{1}{2} \sqrt{\nu_Q^2 - 2\nu_0\nu_Q(1+K_\perp) + 4\nu_0^2(1+K_\perp)^2} \\ & + \frac{1}{2} \sqrt{\nu_Q^2 + 2\nu_0\nu_Q(1+K_\perp) + 4\nu_0^2(1+K_\perp)^2} \\ & - \nu_0(1+K_\perp), \end{aligned} \quad (6)$$

where  $\nu_\perp$  is the horn frequency. One can measure these parameters with high precision since they are all determined from point by point line shapes.<sup>11</sup> We estimate that our uncertainty in the total magnetic shift is  $\pm 0.010\%$  (this is in units of percent of  $\nu$ , i.e.,  $\Delta \nu/\nu$ ). The Knight-shift data  $K_\perp^S$  are shown in Fig. 7. In this plot, we have subtracted the orbital shift  $K^{\text{orb}} = 0.289\%$  as reported in Ref. 2. Our data agree quantitatively with the data of Zimmermann *et al.*<sup>2</sup>

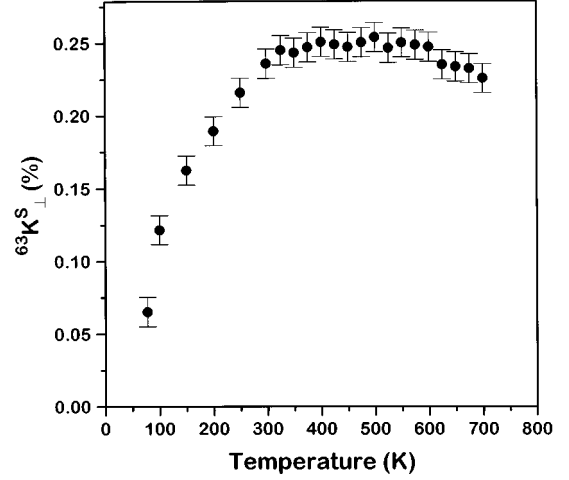


FIG. 7. The measured  $^{63}\text{Cu}(2)$  Knight shift in the perpendicular direction as a function of temperature when the static magnetic field is perpendicular to the crystal  $c$  axis. A temperature-independent orbital contribution has been subtracted off, as given in Ref. 2.

within their quoted precision  $\pm 0.032\%$ , except for temperatures greater than  $\sim 475$  K, above which our data appear to reach a maximum rather than increase monotonically.

## RESULTS AND DISCUSSION

The quantities  $T_1$ ,  $T_{2G}$ , and  $K^S$  reveal important properties of the electronic spin system in the normal state of the cuprates. Based on the Mila-Rice<sup>9</sup> one-component model of the interaction of the copper nuclear spins with the local electronic spin density, one can derive expressions for these quantities:<sup>12</sup>

$$^{63}K_\perp^S(T) = \frac{(A_\perp + 4B)}{\gamma_n \gamma_e \hbar^2} \chi_0(T), \quad (7)$$

$$^{63}T_{1\beta}^{-1} = \frac{k_B T}{2\mu_B^2 \hbar} \lim_{\omega \rightarrow 0} \sum_{\mathbf{q}} ^{63}F_{\beta}(\mathbf{q}) \frac{\chi''(\mathbf{q}, \omega)}{\hbar \omega}, \quad (8)$$

$$\begin{aligned} ^{63}T_{2G}^{-2} = & \frac{0.69}{128\hbar^2} \left[ \frac{1}{N} \sum_{\mathbf{q}} ^{63}F_{\text{eff}}(\mathbf{q})^2 \chi'(\mathbf{q}, 0)^2 \right. \\ & \left. - \left( \frac{1}{N} \sum_{\mathbf{q}} ^{63}F_{\text{eff}}(\mathbf{q}) \chi'(\mathbf{q}, 0) \right)^2 \right], \end{aligned} \quad (9)$$

where  $A_\perp$  and  $B$  are the hyperfine coupling constants, and  $^{63}F_{\beta, \text{eff}}$  are the form factors for the copper nuclei, as discussed in Ref. 4.  $\chi'(\mathbf{q}, \omega)$  is the real part of the dynamical electron-spin susceptibility at wave vector  $\mathbf{q}$  and frequency  $\omega$ , and  $\chi''(\mathbf{q}, \omega)$  is the imaginary part. The expressions for  $T_1$  and  $T_{2G}$  can be simplified considerably by using the Millis, Monien, and Pines (MMP) form for the susceptibility<sup>13</sup> [see Eq. (15) below] and assuming that the correlation length  $\xi$  is large compared to the lattice constant. One then obtains

$$^{63}T_1 T = (132 \text{ s K/eV}^2) \frac{\omega_{\text{sf}}}{\alpha}, \quad (10)$$

$$\left(\frac{1}{63T_{2G}}\right)_{\text{NMR}} = (295 \text{ eV/s})\alpha\xi, \quad (11)$$

where  $\omega_{\text{sf}}$  is the characteristic energy of the spin fluctuations,  $\alpha$  is a parameter in the MMP susceptibility given by  $\chi_Q/\xi^2$ , and  $\chi_Q$  is the susceptibility at  $\mathbf{Q}=(\pi/a, \pi/a)$ . These forms have no assumptions about the temperature dependences of the parameters  $\alpha$ ,  $\omega_{\text{sf}}$ , and  $\xi$ . Note that Eq. (11) was derived for the NMR  $T_{2G}$ , but for NQR one has<sup>14</sup>

$$\left(\frac{1}{T_{2G}}\right)_{\text{NQR}} = \frac{\sqrt{2}}{1.03} \left(\frac{1}{T_{2G}}\right)_{\text{NMR}}. \quad (12)$$

An extensive body of theoretical<sup>4,15</sup> and experimental work<sup>3,16</sup> has provided evidence for the magnetic scaling behavior in the normal state of the doped cuprates, expressed in terms of a relationship between  $\omega_{\text{sf}}$  and  $\xi$ :  $\omega_{\text{sf}} \sim \xi^{-z}$ . Recently Barzykin and Pines (BP) proposed a phase diagram for the magnetic behavior in these materials as a function of planar hole doping and temperature. They identify two crossover temperatures,  $T^*$  and  $T_{\text{cr}}$ , which vary with doping. They propose that between  $T^*$  and  $T_{\text{cr}}$  one should find a possibly nonuniversal,  $z=1$  scaling regime, subsequently termed pseudoscaling by Pines, characterized by  $\omega_{\text{sf}} \sim \xi^{-1} \sim T$ . At temperatures below  $T^*$ , the ‘‘pseudogap’’ regime, the correlation length  $\xi$  saturates at some finite value, while  $\omega_{\text{sf}}$  reaches a minimum and then starts to increase with decreasing temperature. Above  $T_{\text{cr}}$  the system exhibits nonuniversal,  $z=2$  mean-field behavior characterized by the relation  $\omega_{\text{sf}} \sim \xi^{-2} \sim T$ .

$\text{YBa}_2\text{Cu}_4\text{O}_8$  is especially well suited for studying this phase diagram because it does not lose oxygen at high temperatures as do the  $\text{YBa}_2\text{Cu}_3\text{O}_{7-\delta}$  materials.  $\text{YBa}_2\text{Cu}_4\text{O}_8$  also has a planar hole doping believed to be equivalent to  $\text{YBa}_2\text{Cu}_3\text{O}_{6.8}$ ,<sup>17</sup> which corresponds to a crucial part of the phase diagram proposed by BP. Corey *et al.* recently demonstrated the crossover behavior at  $T^*$ , but there has been no conclusive evidence that a crossover at  $T_{\text{cr}}$  exists. At this temperature, BP claim that the static spin susceptibility,  $\chi_0(T)$ , reaches a maximum, and that  $\xi$  is of the order of two lattice spacings. Now, in the QC scaling regime,  $\omega_{\text{sf}} \propto \xi^{-z}$ , so for  $z=1$  scaling the ratio

$$\frac{T_1 T}{T_{2G}} \propto \omega_{\text{sf}} \xi \quad (13)$$

is independent of temperature. On the other hand, for mean-field  $z=2$  behavior above  $T_{\text{cr}}$ , one expects  $\omega_{\text{sf}} \xi^2$  is constant. Furthermore, BP make the assumption that  $\alpha$  is temperature independent,<sup>18</sup> so the ratio

$$\frac{T_1 T}{T_{2G}^2} \propto \omega_{\text{sf}} \chi_Q = \alpha \omega_{\text{sf}} \xi^2 \quad (14)$$

should be temperature independent above  $T_{\text{cr}}$ . In Figs. 8(a) and 8(b) we show the measured ratios  $T_1 T/T_{2G}$  and  $T_1 T/T_{2G}^2$ , respectively. In Fig. 8(a) the crossover at  $T^*$  is clearly evident at 215 K as  $T_1 T/T_{2G}$  becomes independent of temperature for temperatures above this. Above 500 K, the data appear to increase slightly with temperature, although the effect is subtle. The data on  $T_1 T/T_{2G}^2$  in Fig. 8(b), how-

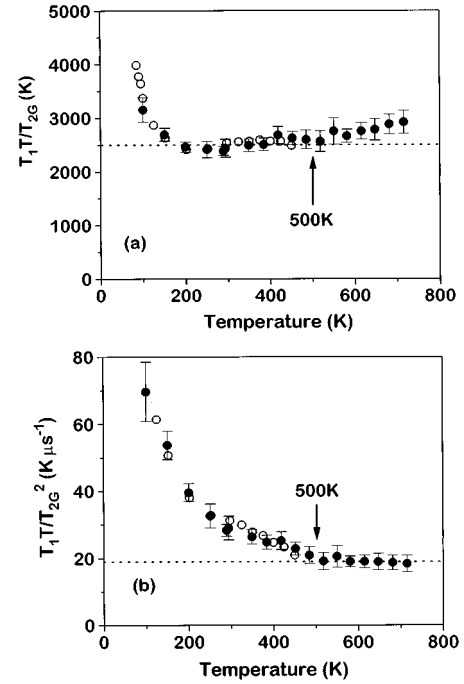


FIG. 8. (a) The NQR  $T_1 T/T_{2G}$  as a function of temperature from about 200 to 500 K, this ratio is independent of temperature. (b) The NQR  $T_1 T/T_{2G}^2$  as a function of temperature. For temperatures above 500 K, this ratio is independent of temperature. Together, (a) and (b) show a crossover in behavior at about 500 K. The open circles are the data of Corey *et al.* (Ref. 3) and the solid circles are the data in the present study. The data shown have not been corrected for the spin-lattice contribution. [Note that these values are calculated using the NQR  $T_{2G}$ , which differs from the NMR case as in Eq. (12).]

ever, show a clear change in behavior at a temperature  $\sim 500$  K. Whereas below this  $T_1 T/T_{2G}^2$  exhibits a strong temperature dependence, above 500 K it is independent of temperature. In the BP model, this change is interpreted as evidence for a crossover to the nonuniversal  $z=2$  mean-field regime of the phase diagram. We note that this change in behavior arises only from a change in slope of  $T_{2G}$ , whereas  $T_1 T$  appears to have a simple linear dependence above 215 K. In fact,  $T_1$  is independent of temperature in this region.

The Knight-shift data provide a second piece of evidence for the existence of an upper temperature crossover. The data in Fig. 7 exhibit a broad maximum at 500 K, the same temperature at which the crossover was noted in the relaxation times. The value of the Knight shift at our highest temperature (715 K) is 90% of the maximum value near 500 K. The 90% point on the low-temperature side of the maximum Knight shift is at 280 K. The average of these two temperatures (498 K) occurs at the temperature of the maximum. Bulk susceptibility measurements on  $\text{YBa}_2\text{Cu}_3\text{O}_{6.84}$  have not shown any evidence for a downturn in the spin susceptibility up to 630 K.<sup>19</sup> Such measurements also include contributions from the copper chain sites which do not necessarily have the same temperature dependence as  $\chi_0(T)$  at the planar sites. On the other hand, in  $\text{La}_{2-x}\text{Sr}_x\text{CuO}_4$ , which does not have a copper chain site, bulk susceptibility measurements<sup>20</sup> have indicated a downturn in  $\chi_0(T)$  at higher temperatures.

For the antiferromagnetic parent compound  $\text{La}_2\text{CuO}_4$ ,

Imai *et al.*<sup>21</sup> found that  $T_1$  and  $T_{2G}$  were well described by the theories of Sokol *et al.*<sup>22</sup> for a Heisenberg antiferromagnet. Moreover, Imai found experimentally that at high temperatures the  $T_1$  was almost independent of doping, so the Heisenberg theory should describe the  $T_1$  of the doped materials at high temperatures. Recently Sokol, Singh, and Elstner<sup>23</sup> (SSE) have found an exact solution for the Heisenberg antiferromagnet and used it to calculate  $T_{2G}$  in terms of the correlation length and the Knight shift with no adjustable parameters. They have proposed that this may also give a good approximation for the lightly doped materials at high temperatures.<sup>24</sup> Accordingly, we have analyzed our data using their expression to deduce the correlation length as a function of temperature. We have also used the BP expression following their hypothesis that  $\xi$  is two lattice spacings at  $T_{cr}$  in order to determine the parameter  $\alpha$ .

The correlation length is extracted by numerically evaluating Eq. (9) for  $T_{2G}$  using a particular form for the susceptibility. The MMP mean-field form

$$\chi(\mathbf{q}, \omega)_{\text{MMP}} = \frac{\chi_0}{1 + (\mathbf{q} - \mathbf{Q})^2 \xi^2 - i\omega/\omega_{sf}}, \quad (15)$$

gives a particularly simple result for large  $\xi$  [see Eq. (11)]. The susceptibility given by SSE for a Heisenberg antiferromagnet is

$$\chi(\mathbf{q}, \omega, T)_{\text{SSE}} = \frac{\chi_0(T)[1 + \theta(T)]}{1 + \theta(T)\gamma(\mathbf{q}) + i\Gamma_q\omega}, \quad (16)$$

where

$$\gamma(\mathbf{q}) = \frac{1}{2} [\cos(q_x a) + \cos(q_y a)], \quad (17)$$

$$\theta(T) = \frac{4\xi^2(T)}{1 + 4\xi^2(T)}, \quad (18)$$

and  $\Gamma_q$  is a characteristic rate which is unimportant for the calculation of  $T_{2G}$ . Note that the MMP formula is valid only for  $\mathbf{q}$  close to the antiferromagnetic wave vector  $\mathbf{Q}$ . If one expands the SSE formula for  $\mathbf{q}$  close to  $\mathbf{Q}$  and for large correlation length one recovers the MMP formula with  $\alpha$  equal to  $8\chi_0(T)$ . The uniform susceptibility,  $\chi_0(T)$ , in this expression is obtained from the Knight shift. One can then fit the  $T_{2G}$  data using Eq. (9), leaving  $\xi(T)$  as the only variable parameter. Since not all of the Knight-shift data points were at the same temperatures as the  $T_{2G}$  data points, a smoothly interpolated value for  $T_{2G}$  was taken.

Curves for  $\xi^{-1}(T)$  are shown in Fig. 9 using the two expressions for the susceptibility. The fit using the SSE expression is represented by the open circles. In contrast to the BP formulation, the SSE expression has no variational parameters and gives a correlation length of  $1.4a$  at 500 K, a value slightly lower than the BP hypothesis of  $2a$ . If one chooses  $\alpha$  in the BP formula such that  $\xi = 1.4a$ , then the correlation lengths determined by the two expressions agree remarkably well. The BP hypothesis that  $\xi = 2a$  at  $T_{cr}$  is based on the assumption that at short correlation length the scaling theory will fail, but whether this occurs at  $\xi = 2a$  or some other value seems somewhat arbitrary and it may be that a value of  $1.4a$  is more realistic. The solid symbols in

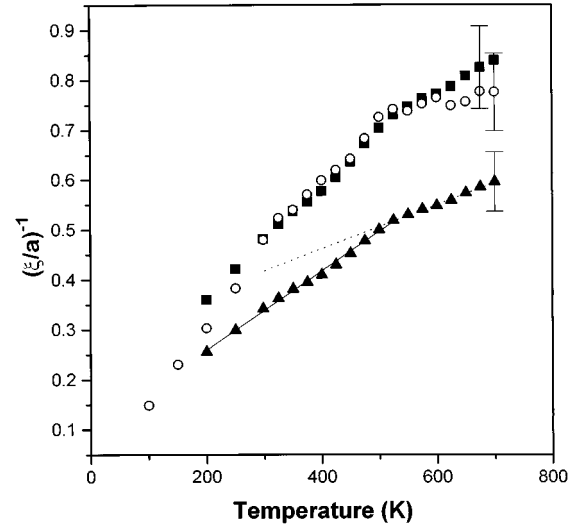


FIG. 9. The calculated inverse correlation length as a function of temperature. The open circles are found using the susceptibility in Eq. (16) due to SSE, the solid triangles are using the susceptibility in Eq. (15) and a value of  $\alpha$  so that  $\xi = 2a$  at 500 K, and the solid squares are using a value of  $\alpha$  so that  $\xi = 1.4a$  at 500 K. The solid and dashed lines are guides to the eye.

Fig. 9 show the fits obtained from the MMP susceptibility using these two values of  $a$ . This agreement suggests that the SSE expression is valid at higher temperatures for the doped yttrium materials. Of course, in analogy to the results of Imai *et al.* in Sr-doped  $\text{La}_2\text{CuO}_4$ , we do not expect the SSE expression to hold at lower temperatures.

Recall that in the pseudoscaling or QC regime (between  $T^*$  and  $T_{cr}$ ) of the BP phase diagram the correlation length is inversely proportional to temperature and above this the square of the correlation length should be inversely proportional to temperature. This change in behavior is clearly seen in Fig. 9. In fact, a better fit to the data (as calculated by the MMP expression such that  $\xi = 2a$  at  $T_{cr}$ ) is obtained by assuming a linear temperature dependence, giving  $(\xi/a)^{-1} = 0.10 + (7.9 \times 10^{-4} \text{ K}^{-1})T$  for  $T < 500$  K, and  $(\xi/a)^{-2} = 0.29 + (4.4 \times 10^{-4} \text{ K}^{-1})T$  for  $T > 500$  K. ( $\xi$  as calculated via the SSE expression exhibits similar behavior).

## CONCLUSIONS

Our measurements of the temperature dependence of  $T_{2G}$  at high temperatures show a crossover in behavior at a temperature  $T_{cr}$  of 500 K. The crossover is clearly expressed by examining the temperature dependence of  $T_1/T_{2G}$  and  $T_1/T_{2G}^2$ . Spin-lattice fluctuations affect the echo decay at higher temperatures, but can easily be corrected for and do not change the temperature dependence of  $T_{2G}$ . Our Knight-shift data also show a broad maximum centered about 500 K. Both results are in agreement with predictions of Barzykin and Pines. Calculations of the correlation length using a theory due to Sokol, Singh, and Elstner indicate that  $\xi$  is of the order of one to two lattice spacings at this crossover temperature, and lend support to the picture developed by Barzykin and Pines about the upper crossover temperature  $T_{cr}$ . Likewise, the agreement with BP supports the hypothesis that the SSE expression is valid at higher temperatures

for at least part of the doping range of the conducting materials. Previous work showed the existence of a lower crossover temperature  $T^*$  below which  $z=1$  scaling no longer held true, but rather  $\xi$  became independent of temperature.

### ACKNOWLEDGMENTS

We are grateful to Victor Barzykin, David Pines, Alexander Sokol, and Andrey Chubukov for many illuminating discussions. We thank Dr. M. Takigawa for pointing out an error in two of our equations in an earlier version of the paper. We also wish to thank Dylan Smith and Craig Milling for help in taking the data, and Bob Corey and Raivo Stern for discussions of their previous work. This work has been supported by the Science and Technology Center for Superconductivity under NSF Grant No. DMR91-20000 (CPS, NC, BD, TI) and the U.S. DOE Division of Materials Research under Grant No. DEFG02-91ER45439 (CPS, NC).

### APPENDIX

The Gaussian component  $T_{2G}$  of the spin-echo decay in the high-temperature superconductors traditionally has been evaluated under the assumption that the neighboring spins remain static. Walstedt and Cheong<sup>25</sup> demonstrated that dynamical effects are important for  $^{63,65}\text{Cu}$  and  $^{17}\text{O}$  decay in  $\text{La}_{1.85}\text{Sr}_{0.15}\text{CuO}_4$ . Recently Recchia, Gorny, and Pennington<sup>26</sup> and Keren *et al.*<sup>27</sup> have shown that in  $\text{YBa}_2\text{Cu}_3\text{O}_7$  the echo decays for  $^{89}\text{Y}$  and  $^{17}\text{O}$  are dominated by coupling to the Cu nuclei which are modulated in time by the spin-lattice fluctuations of the Cu nuclei. Here we evaluate the effect of the Cu  $T_1$  on the Cu  $T_{2G}$  in  $\text{YBa}_2\text{Cu}_4\text{O}_8$  showing that the correction can be obtained and that it is small. We apply a generalization of the analysis of Recchia *et al.* to the  $^{63}\text{Cu}$  decay in which the planar Cu are coupled indirectly to both like (same isotope) and unlike (other isotope) nuclei in the plane.

The Hamiltonian for the indirectly coupled spins is<sup>28</sup>

$$H = \sum_{\mathbf{r}_1, \mathbf{r} \neq 0} \hbar a_z(\mathbf{r}) I_z(\mathbf{r}_1) I_z(\mathbf{r}_1 + \mathbf{r}) + \frac{\hbar a_\perp}{2} [I_+(\mathbf{r}_1) I_-(\mathbf{r}_1 + \mathbf{r}) + I_-(\mathbf{r}_1) I_+(\mathbf{r}_1 + \mathbf{r})], \quad (\text{A1})$$

where  $a_z$  and  $a_\perp$  are the parallel and perpendicular indirect coupling constants.<sup>29</sup> No analytic expression exists for the echo decay for such a Hamiltonian for the general case. Pennington and Slichter showed that frequently  $a_\perp \ll a_z$  for the high-temperature superconductors, in which case the problem is simplified. Assuming that spin-lattice relaxation is much slower than the echo decay (the static approximation), the echo decay is Gaussian with decay constant:

$$\left( \frac{1}{\eta T_{2G}^2} \right)_{\text{NMR}} = \frac{\eta P}{8} \sum_{\mathbf{r} \neq 0} a_z(\mathbf{r})^2, \quad (\text{A2})$$

where  $\eta P$  is the natural abundance of the nucleus  $\eta$  ( $\eta = 63$  or  $65$  denotes the two Cu isotopes).

Validity of the static assumption requires that the spin-lattice relaxation time of the Cu nuclei be long and that mutual spin flips between Cu neighbors be infrequent. Here we

show that in our case there is a small correction since at higher temperatures  $T_1 \sim 600 \mu\text{s}$  and  $T_{2G} \sim 150 \mu\text{s}$ .

Recchia *et al.* showed that in the Gaussian-approximation formalism the echo height is given by  $M(2\tau) = M_0 e^{-\langle \phi^2 \rangle / 2}$ , where  $\langle \phi^2 \rangle$  is the mean-square phase angle accumulated by the spins in the rotating frame after a  $\pi/2 - \tau - \pi - \tau$  sequence. The phase angle of a particular nucleus is given by the time integral of the local field. We take the local field to be given by the indirect couplings to the other Cu nuclei in the plane. For a single coupling, the local field is

$$h_z(t) = \frac{-1}{\gamma} a_z(\mathbf{r}) \sum_m m p_m(t), \quad (\text{A3})$$

where  $m$  is the  $I_z$  quantum number and  $p_m(t)$  is one if the state is occupied and zero if not. The  $\pi$  pulse at time  $\tau$  has two effects. First, it acts as though it changed the direction of precession for the observed field nucleus, which effectively changes the sign of the local field  $h_z(t)$  and hence the sign of the phase accumulated for  $t > \tau$ . Thus,

$$\phi(2\tau) = \gamma \int_0^\tau h_z(t) dt - \gamma \int_\tau^{2\tau} h_z(t) dt. \quad (\text{A4})$$

Secondly, it redistributes the populations of the levels depending on whether the coupling nucleus is like or unlike, whether NMR or NQR is employed, and in the case of NMR, which transition is observed. For NMR in which the central transition is observed the  $\pi$  pulse redistributes like nuclei according to

$$p_{+1/2}(\tau^+) = p_{-1/2}(\tau^-), \quad p_{+3/2}(\tau^+) = p_{+3/2}(\tau^-), \quad (\text{A5})$$

$$p_{-1/2}(\tau^+) = p_{+1/2}(\tau^-), \quad p_{-3/2}(\tau^+) = p_{-3/2}(\tau^-),$$

and for NQR the  $\pi$  pulse redistributes like nuclei according to

$$p_{+1/2}(\tau^+) = p_{+3/2}(\tau^-), \quad p_{+3/2}(\tau^+) = p_{+1/2}(\tau^-), \quad (\text{A6})$$

$$p_{-1/2}(\tau^+) = p_{-3/2}(\tau^-), \quad p_{-3/2}(\tau^+) = p_{-1/2}(\tau^-).$$

For unlike nuclei, the populations are not redistributed. To calculate  $\langle \phi^2 \rangle$ , one must take the square of Eq. (A4) and take the thermal average:

$$\langle \phi^2 \rangle = \left\langle \int_0^\tau \int_0^\tau - \int_0^\tau \int_\tau^{2\tau} - \int_\tau^{2\tau} \int_0^\tau \right. \\ \left. + \int_\tau^{2\tau} \int_\tau^{2\tau} \sum_{m, m'} a_z^2(\mathbf{r}) m m' p_m(t) p_{m'}(t') dt dt' \right\rangle, \quad (\text{A7})$$

where we take  $\langle p_m(t) p_{m'}(t') \rangle = P_{mm'}(|t-t'|)/4$ .  $P_{mm'}(t)$  is the probability that if a nucleus is in the state  $m$  at time  $t=0$  then it is in state  $m'$  at time  $t$ . These probabilities are determined from the normal modes for spin-lattice relaxation. The time dependence of the  $p_m(t)$  are given by

$$\frac{dp_m(t)}{dt} = \sum_n W_{mn} P_n(t), \quad (\text{A8})$$

where

$$\mathbf{W} = \frac{W_1}{3} \begin{pmatrix} -3 & 3 & 0 & 0 \\ 3 & -7 & 4 & 0 \\ 0 & 4 & -7 & 3 \\ 0 & 0 & 3 & -3 \end{pmatrix}. \quad (\text{A9})$$

Here we use the quantity  $W_1 = 3/(2T_1)$ . By transforming to a basis  $\vec{q} = \mathbf{R}^{-1}\vec{p}$ , where  $\mathbf{R}$  is the matrix of normalized eigenvectors of  $\mathbf{W}$ , one can determine the normal modes of the spin-lattice relaxation. Then by choosing the initial conditions such that the system is in that state  $i$ , one can show that the probability that it will make a transition to the state  $j$  is given by

$$P_{ij}(t) = \sum_m R_{jm} R_{mi}^{-1} e^{\lambda_m t}, \quad (\text{A10})$$

where  $\lambda_m$  is the eigenvalue of the  $m$ th normal mode ( $\lambda_1 = 0$ ,  $\lambda_2 = -2W_1/3$ ,  $\lambda_3 = -2W_1$ ,  $\lambda_4 = -4W_1$ ).

Equation (A7) above gives the contribution for a single coupled nucleus, but in fact there are couplings to all the nuclei in the plane. We assume the local field seen by the observed nucleus is the sum over all the indirectly coupled sites, and that at each site there is 69%  $^{63}\text{Cu}$  and 31%  $^{65}\text{Cu}$ . Furthermore, each site fluctuates independently, so each coupling contributes independently to  $\langle \phi^2 \rangle$ . Performing the integrals in Eq. (A7), summing over all sites and employing Eqs. (A2), (A3), (A5), (A6), and (A10), and denoting  $\eta$  for the nucleus under observation, and  $\eta'$  for the other isotope we obtain for NMR

$$\ln\left(\frac{M}{M_0}\right) = \frac{-1}{(\eta W_1 \eta T_{2G})^2} \left( \frac{9}{4} \left[ \frac{40}{3} \eta W_1 \tau - 8 e^{-4\eta W_1 \tau/3} + 36 e^{-2\eta W_1 \tau/3} - 28 \right] + \frac{-18}{(\eta' W_1 \eta T_{2G})^2} \left( \frac{\eta' P}{\eta P} \right) \right) \times \left( \frac{\eta' \gamma}{\eta \gamma} \right)^2 \left[ 5 \eta' W_1 \tau/3 + 5 e^{-2\eta' W_1 \tau/3} - \frac{5}{4} e^{-4\eta' W_1 \tau/3} - \frac{15}{4} \right], \quad (\text{A11})$$

and for NQR

$$\ln\left(\frac{M}{M_0}\right) = \frac{-1}{(\eta W_1 \eta T_{2G})^2} \left[ 15 \eta W_1 \tau + 36 e^{-2\eta W_1 \tau/3} - \frac{27}{4} e^{-4\eta W_1 \tau/3} - \frac{117}{4} \right] + \frac{-18}{(\eta' W_1 \eta T_{2G})^2} \left( \frac{\eta' P}{\eta P} \right) \times \left( \frac{\eta' \gamma}{\eta \gamma} \right)^2 \left[ \frac{5}{3} \eta' W_1 \tau + 5 e^{-2\eta' W_1 \tau/3} - \frac{5}{4} e^{-4\eta' W_1 \tau/3} - \frac{15}{4} \right]. \quad (\text{A12})$$

For  $W_1 \tau \ll 1$  the right-hand side of the equations reduce to the form  $f(2\tau) \exp(-(2\tau)^2/2T_{2G}^2)$ . The function  $f(2\tau)$  is given by

$$-\ln f(2\tau) = \eta C_1 \eta W_1 \frac{(2\tau)^3}{\eta T_{2G}^2} + \eta C_2 \eta W_1^2 \frac{(2\tau)^4}{\eta T_{2G}^2}, \quad (\text{A13})$$

where  $^{63}C_1 = 0.7177$ ,  $^{63}C_2 = -0.2008$ ,  $^{65}C_1 = 1.3276$ , and  $^{65}C_2 = -0.3109$  for NMR, and  $^{63}C_1 = 0.2755$ ,  $^{63}C_2 = -0.0830$ ,  $^{65}C_1 = 0.5804$ , and  $^{65}C_2 = -0.1393$ , for NQR. Here we have utilized the relation  $^{65}W_1 = (^{65}\gamma/^{63}\gamma)^2 ^{63}W_1$ . Note that in these expressions the factor of  $\sqrt{2}$  between the NQR and NMR  $T_{2G}$  comes out naturally and has been accounted for.

All the parameters in this expression are known, so including  $f(2\tau)$  in Eq. (1) only introduces a correction to the fitted value for  $T_{2G}$ . We find that for our case (NQR of  $^{63}\text{Cu}$ ) this correction is at most  $\sim 10\%$  for  $^{63}\text{Cu}$  at the higher temperatures, but at lower temperatures where  $T_1$  is longer the correction is smaller. Furthermore the correction is smaller for the  $^{63}\text{Cu}$  than for the  $^{65}\text{Cu}$ . We show the corrected and uncorrected  $T_{2G}$  in Fig. 10.

It is interesting to note that the correction is much smaller for NQR than for NMR, reflecting the fact that in NQR there are twice as many like nuclei. A  $T_1$  fluctuation for a like

nucleus *slows down* the echo decay whereas for an unlike nucleus a  $T_1$  fluctuation *increases* the echo decay rate. The dephasing caused by a static like nucleus is not refocused by the  $\pi$  pulse, which gives rise to the static  $T_{2G}$ . But if the

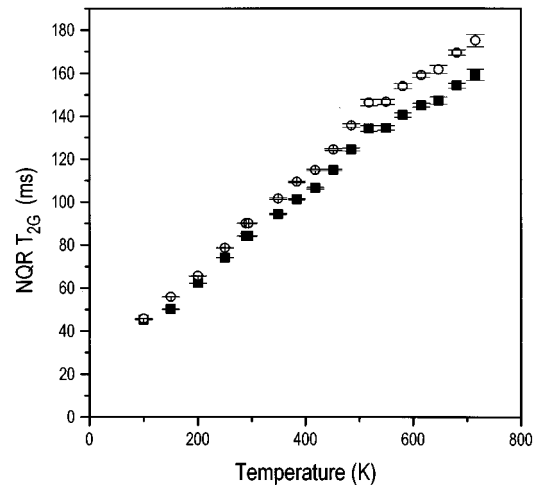


FIG. 10. The NQR  $T_{2G}$  as a function of temperature showing the effects of correcting for the spin-lattice relaxation contribution. The solid squares are the uncorrected values, and the open circles are the corrected values. Note that the correction is smaller at lower temperatures.

coupled like nucleus undergoes a  $T_1$  fluctuation, the observed nucleus will not dephase as much as it would if the coupled nucleus were static. For unlike nuclei any  $T_1$  fluctuation will increase the echo decay rate, since in the static case the unlike nuclei couplings are refocused. In both NMR and NQR, the effects of  $T_1$  fluctuations of like and unlike nuclei partially cancel each other. It happens that for NQR the  $T_1$  fluctuations are more effectively canceled because there are more like nuclei.

It has been argued that the  $a_{\perp}$  term in Eq. (A1), which gives rise to flip-flop processes, is important in  $\text{La}_{1.85}\text{Sr}_{0.15}\text{CuO}_4$  (see Ref. 25). We argue that the flip-flop term is suppressed for the Cu in  $\text{YBa}_2\text{Cu}_4\text{O}_8$ . There are two reasons. We will discuss the case for NMR of the  $+1/2$  to  $-1/2$  transition. In order for two nuclei to undergo a mutual spin flip, they must be able to conserve energy. The two nuclei must be like nuclei, and the local fields at two nuclei must also be similar. Consider then mutual spin flips between nearest-neighbor nuclei which we designate as I and

II. Each has three other nearest neighbors, each of which can be in one of four nuclear levels. Thus, there is very little chance that nuclei I and II have the same local fields. In fact, if one assumes that I and II are in the  $\pm 1/2$  levels and are each coupled to the three next-nearest neighbors, the probability that I and II will have identical local fields is only  $\sim 14\%$ .

The second argument for the suppression of mutual spin flips is the following. If one has mutual spin flips, this process should happen randomly and have a correlation time associated with it. Recchia *et al.* studied the echo decay for the Y in  $\text{YBa}_2\text{Cu}_3\text{O}_7$ . We expect the ratio  $a_z/a_{\perp}$  to be large for this material. They show that the Y echo decay results from flips of the Cu nuclei. They found that they could fit their data exactly using only the spin-lattice fluctuations of the planar Cu to limit its lifetime in a state. One would expect that if mutual spin flips between the planar Cu were indeed important then the Y echo decay would have an extra component associated with the correlation time for spin flips.

\* Also at Department of Chemistry, University of Illinois at Urbana-Champaign, Urbana, IL.

<sup>1</sup>Y. Itoh, H. Yasuoka, Y. Fujiwara, Y. Ueda, T. Machi, I. Tomeno, K. Tai, N. Koshizuka, and S. Tanaka, *J. Phys. Soc. Jpn.* **61**, 1287 (1992).

<sup>2</sup>R. Stern, M. Mali, J. Roos, and D. Brinkmann, *Phys. Rev. B* **51**, 15 478 (1995); M. Bankay, M. Mali, J. Roos, and D. Brinkmann, *ibid.* **50**, 6416 (1994); H. Zimmermann, M. Mali, M. Bankay, and D. Brinkmann, *Physica C* **185–189**, 1145 (1991).

<sup>3</sup>R. L. Corey, N. J. Curro, K. O'Hara, T. Imai, C. P. Slichter, K. Yoshimura, M. Katoh, and K. Kosuge, *Phys. Rev. B* **53**, 5907 (1996).

<sup>4</sup>V. Barzykin and D. Pines, *Phys. Rev. B* **52**, 13 585 (1995).

<sup>5</sup>J. Sok, M. Xu, W. Chen, B. J. Suh, J. Gohng, D. K. Finnemore, M. J. Kramer, L. A. Schwartzkopf, and B. Dabrowski, *Phys. Rev. B* **51**, 6035 (1995).

<sup>6</sup>M. Bankay, M. Mali, J. Roos, I. Mangelschots, and D. Brinkmann, *Phys. Rev. B* **46**, 11 228 (1992).

<sup>7</sup>T. P. Das and E. L. Hahn, *Nuclear Quadrupole Resonance Spectroscopy* (Academic, New York, 1958), Suppl. 1, p. 77; T. P. Das and A. K. Saha, *Phys. Rev.* **98**, 516 (1955); Also see Ref. 3. Small ambient fields cause a modulation of the NQR echo envelope, hence reducing the Gaussian decay by an amount proportional to the frequency of this modulation,  $\gamma B$ .

<sup>8</sup>C. Milling *et al.* (unpublished).

<sup>9</sup>F. Mila and T. M. Rice, *Physica C* **157**, 561 (1989).

<sup>10</sup>C. P. Slichter, *Principles of Magnetic Resonance*, 3rd ed. (Springer-Verlag, New York, 1990).

<sup>11</sup>Note that the shift was measured in a nitrogen atmosphere whereas the NQR frequency was measured in air. It has been observed that in the Sr-doped 214 materials the quadrupole coupling changes slightly depending on the atmosphere.

<sup>12</sup>For a discussion of these derivations, see Refs. 3 and 4.

<sup>13</sup>A. J. Millis, H. Monien, and D. Pines, *Phys. Rev. B* **42**, 167 (1990).

<sup>14</sup>T. Imai, C. P. Slichter, K. Yoshimura, M. Katoh, and K. Kosuge,

*Phys. Rev. Lett.* **71**, 1254 (1993).

<sup>15</sup>S. Chakravarty, B. I. Halperin, and D. R. Nelson, *Phys. Rev. B* **39**, 2344 (1989); A. Chubukov and S. Sachdev, *Phys. Rev. Lett.* **71**, 169 (1993); V. Barzykin, D. Pines, A. Sokol, and D. Thelen, *Phys. Rev. B* **49**, 1544 (1994); A. Sokol and D. Pines, *Phys. Rev. Lett.* **71**, 2813 (1993).

<sup>16</sup>For a recent review, see C. P. Slichter, in *Strongly Correlated Electron Systems*, edited by K. S. Bedell *et al.* (Addison-Wesley, Reading, MA, 1994), p. 427.

<sup>17</sup>See Z. P. Han, R. Dupree, A. Gencten, R. S. Liu, and P. P. Edwards, *Phys. Rev. Lett.* **69**, 1256 (1992). The assumption is based on  $^{89}\text{Y}$  NMR shifts.

<sup>18</sup>Justification for this assumption can be found in the self-consistent renormalization theory of spin fluctuations. For a review see T. Moriya, *J. Magn. Magn. Mater.* **14**, 1 (1979).

<sup>19</sup>J. M. Tranquada, A. H. Moudden, A. I. Goldman, P. Zolliker, D. E. Cox, G. Shirane, S. K. Sinha, D. Vaknin, D. C. Johnston, M. S. Alvarez, A. J. Jacobson, J. T. Lewandowski, and J. M. Newsam, *Phys. Rev. B* **38**, 2477 (1988).

<sup>20</sup>D. Johnston *et al.*, *Phys. Rev. Lett.* **62**, 957 (1989); R. Yoshizaki *et al.*, *Physica C* **166**, 417 (1990).

<sup>21</sup>T. Imai, C. P. Slichter, K. Yoshimura, and K. Kosuge, *Phys. Rev. Lett.* **70**, 1002 (1993).

<sup>22</sup>A. Sokol *et al.*, *Phys. Rev. Lett.* **72**, 1549 (1994).

<sup>23</sup>A. Sokol, R. P. P. Singh, and N. Elstner, *Phys. Rev. Lett.* **76**, 4416 (1990).

<sup>24</sup>A. Sokol (private communication).

<sup>25</sup>R. E. Walstedt and S.-W. Cheong, *Phys. Rev. B* **51**, 3163 (1995).

<sup>26</sup>C. H. Recchia, K. Gorny, and C. H. Pennington, *Phys. Rev. B* **54**, 4207 (1996).

<sup>27</sup>A. Keren, H. Alloul, P. Mendels, and Y. Yoshinara, *Phys. Rev. Lett.* **78**, 3547 (1997).

<sup>28</sup>C. H. Pennington and C. P. Slichter, *Phys. Rev. Lett.* **66**, 381 (1991).

<sup>29</sup>For a calculation of these couplings see Ref. 29 and also D. Thelen and D. Pines, *Phys. Rev. B* **49**, 3528 (1994).